

# ATLAS History, Operations and Data Processing

Larry Denneau, Jr.

John Tonry

Henry Weiland

Amanda Lawrence

Robert Siverd, Jr.

March 12, 2024



# Contents

<b>1</b>	<b>Introduction</b>	<b>3</b>
<b>2</b>	<b>History of the ATLAS Survey</b>	<b>3</b>
<b>3</b>	<b>Facilities</b>	<b>4</b>
3.1	ATLAS-Haleakalā, Haleakalā, Maui. MPC observatory code T05. . . . .	4
3.2	ATLAS-Maunaloa, Maunaloa, Hawai'i. MPC observatory code T08. . . . .	5
3.3	ATLAS-Chile, El Sauce Observatory, Rio Hurtado, Chile. MPC observatory code W68. . . . .	5
3.4	ATLAS-South Africa, Sutherland Observing Station, South Africa. MPC observatory code M22. . . . .	6
3.5	Future Facilities . . . . .	7
3.6	Collaborators . . . . .	7
<b>4</b>	<b>ATLAS Data Reduction Pipeline</b>	<b>8</b>
4.1	Overview . . . . .	8
4.2	Data Reduction . . . . .	9
4.3	Image Subtraction . . . . .	11
4.4	Post-Reduction and Deep Source Detection . . . . .	13
4.5	Asteroid Processing . . . . .	13
4.6	Forced Photometry Server . . . . .	14

# 1 Introduction

This document provides an overview of telescope operations, data reduction software, and data products produced by the Asteroid Terrestrial-Impact Last Alert System (ATLAS)[1]. ATLAS is a NASA-funded, ground-based robotic survey for near-Earth objects (NEOs) constructed and operated by the University of Hawai‘i. ATLAS is a “wide and shallow” survey that specializes in rapid all-sky coverage and detection of asteroids on final impact or near-miss trajectories. NASA projects are mandated to make their data products available to the public. To meet that requirement, ATLAS is publishing its pipeline-reduced image data and source detection catalogs to the NASA Planetary Data System (PDS) Small Bodies Node (SBN) archive. ATLAS astrometric measurements of asteroids are separately published in near real-time to the International Astronomical Union (IAU) Minor Planet Center (MPC). Users looking for submitted asteroid data are encouraged to visit the MPC archives.

As of April 2022, ATLAS operates four essentially-identical telescopes around the world to uniformly scan the night sky for unknown asteroids. These telescopes are located in South Africa, Chile, and two in Hawai‘i. Each telescope consists of a 0.5 m Wright-Schmidt optical tube assembly that images 28 square degrees on the sky onto an STA 1600 10K x 10K CCD, achieving a pixel scale of 1.86 arcseconds. A typical 30-second ATLAS exposure reaches a  $5-\sigma$  detection sensitivity of  $V = 19.7$  in dark conditions. Observations are usually executed using one of the ATLAS wideband optical filters: cyan (or “c”, 420-650 nm) when the moon is down, and orange (or “o”, 560-820 nm) when the moon is up.

## 2 History of the ATLAS Survey

The concept for a replicable, high-speed all-sky survey capable of contributing to the discovery and detection of hazardous asteroids was described in [1]. This concept was proposed to NASA ROSES in 2013 in service of the U.S. Congressional NEO mandate to catalog 90% of the estimated population of NEOs larger than 140 meters and to provide warning for small ( $< 1$  km diameter) asteroids on final impact trajectories with the Earth.

In 2013, NASA awarded a grant to the University of Hawai‘i’s John Tonry, Larry Denneau and Robert Jedicke, all veterans of the Pan-STARRS sky survey [2], to develop the ATLAS concept and build two telescope units. After a competitive design solicitation, the selected design specified a 0.5 m,  $f/2$  Wright-Schmidt telescope with a 28 square degree field-of-view capable of reaching magnitude 19.7 on dark nights. The telescopes were sited at the Hawai‘ian summits of Haleakalā and Maunaloa, with Haleakalā coming online in 2015 and Maunaloa in 2017. The two facilities are fully robotic and dedicate their entire nights to surveying the sky for incoming asteroids.

In 2019, following several years of successful operation of the Hawai‘i facilities, Co-PIs Tonry and Denneau proposed via NASA ROSES for funds to augment the ATLAS system with two additional telescopes in the southern hemisphere. Completion of these telescopes allows full “pole-to-pole” coverage of the entire sky, every night, if weather is clear. These telescopes are essentially identical copies of the original Hawai‘i ATLAS telescopes, with minor changes introduced by vendors for the optical tube assembly and telescope mount. Construction of these facilities was delayed by COVID-19 issues, but in late 2021, commissioning began on ATLAS telescopes at Sutherland Observing Station in South Africa and in January 2022 at El Sauce Observatory in Rio Hurtado, Chile. Table 1 summarizes the existing ATLAS telescope locations and the operational history.

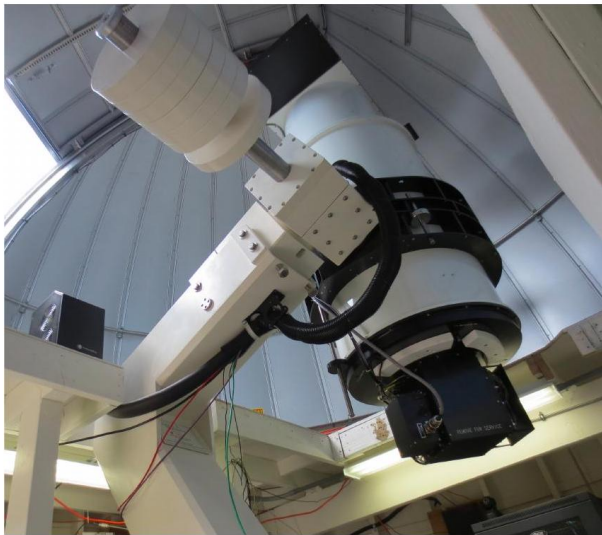
ATLAS Site ID	Location	MPC Code	Start Date	MJD	Elevation (m)	Clear Nights per Year
01	Maunaloa, Hawai'i	T08	February 2017	57794	3429	315
02	Haleakalā, Maui	T05	June 2015	59666	3041	315
03	Sutherland Observing Station, South Africa	M22	December 2021	59561	1764	300
04	El Sauce Observatory, Rio Hurtado, Chile	W68	January 2022	59605	1609	320
05	Tenerife, Canary Islands	TBD	TBD	TBD	2393	300

Table 1: Current and planned locations for ATLAS telescopes

### 3 Facilities

#### 3.1 ATLAS-Haleakalā, Haleakalā, Maui. MPC observatory code T05.

Haleakalā, which means “house of the sun” in Hawai’ian, is home to numerous world-class astronomical facilities, most prominently the 4-meter Daniel K. Inouye solar telescope. The Haleakalā High-Altitude Observatory has been in operation since 1961. ATLAS has NEO finders Pan-STARRS 1 and Pan-STARRS 2 as its neighbors.



MPC Site	Aperture Diameter	Latitude	Longitude	Altitude	Datum
T05	0.5-m	20.7075°N	-156.257°E	3039 m	WGS84

Dates	Name	Type	Pixel Scale	Field of View	Datum
2015 on	STA-1600	Imager	1.86 arcsec	28 deg <sup>2</sup>	Imaging Technology Laboratories 10.5K x 10.5K CCD; STA1600LN_10.5K detector; cyan, orange, and red filters; bi-parting blade shutter

### 3.2 ATLAS-Maunaloa, Maunaloa, Hawai‘i. MPC observatory code T08.

ATLAS is located at the NOAA Global Monitoring Laboratory’s site on the north flank of active Maunaloa volcano on Hawai‘i’s Big Island. This NOAA facility has been monitoring atmospheric change since the 1950s. ATLAS occupies the dome of a former solar telescope that has been repurposed for nighttime observing.



MPC Site	Aperture	Latitude	Longitude	Altitude	Datum
T08	0.5-m	19.5362°N	-155.5763°E	3397 m	WGS84

Dates	Name	Type	Pixel Scale	Field of View	Datum
2017 on	STA-1600	Imager	1.86 arcsec	28 deg <sup>2</sup>	Imaging Technology Laboratories 10.5K x 10.5K CCD; STA1600LN_10.5K detector; cyan, orange, and red filters; bi-parting blade shutter

### 3.3 ATLAS-Chile, El Sauce Observatory, Rio Hurtado, Chile. MPC observatory code W68.

Observatorio El Sauce (“The Willow Tree”) hosts telescopes for planetary defense, science, astrophotography, and space situational awareness. Operational since 2015, El Sauce is a fully robotic facility located in the Río Hurtado Valley, in the south of the Atacama desert, with some of the best observing conditions in the world.



MPC Site	Aperture	Latitude	Longitude	Altitude	Datum
W68	0.5-m	30.47103°S	-70.76498°E	1609.6 m	WGS84

Dates	Name	Type	Pixel Scale	Field of View	Datum
2022 on	STA-1600	Imager	1.86 arcsec	28 deg <sup>2</sup>	Imaging Technology Laboratories 10.5K x 10.5K CCD; STA1600LN_10.5K detector; cyan, orange, and red filters; bi-parting blade shutter

### 3.4 ATLAS-South Africa, Sutherland Observing Station, South Africa. MPC observatory code M22.

Located in South Africa's Karoo region near the town of Sutherland, the South African Astronomical Observatory's Sutherland Station hosts many world-class astronomical telescopes, most prominently the 11 m South African Large Telescope (SALT).



MPC Site	Aperture	Latitude	Longitude	Altitude	Datum
M22	0.5-m	32.380461°S	20.810317°E	1764 m	WGS84

Dates	Name	Type	Pixel Scale	Field of View	Datum
2021 on	STA-1600	Imager	1.86 arcsec	28 deg <sup>2</sup>	Imaging Technology Laboratories 10.5K x 10.5K CCD; STA1600LN_10.5K detector; cyan, orange, and red filters; bi-parting blade shutter

### 3.5 Future Facilities

ATLAS #5 has been proposed and funded by the Instituto de Astrofísica de Canarias and is on schedule for completion in late 2022 or early 2023. Aided by recent detector and optical improvements, this system will be a departure from the ATLAS 0.5 m Wright-Schmidt design and will more closely resemble the concept in Tonry et al. 2011 — multiple inexpensive apertures co-mounted and co-pointed to achieve sky coverage and depth, at a cost well below an ATLAS telescope for similar pixel scale and performance.

### 3.6 Collaborators

The ATLAS system relies on in-kind contributions from the following collaborating institutions for real-time review of near Earth asteroid discoveries, data redundancy, and auxiliary scientific output:

- Queen's University Belfast
- South African Astronomical Observatory
- Millennium Institute of Astrophysics, Chile
- Obstech SpA
- Universidad de Chile

## 4 ATLAS Data Reduction Pipeline

### 4.1 Overview

ATLAS image data are reduced at each telescope in real-time for immediate feedback regarding telescope performance. The raw and reduced data products are streamed to the University of Hawai‘i datacenter in Mānoa for image subtraction and asteroid detection. Each telescope includes an auxiliary wide-field 35mm camera that is co-pointed with each main exposure. To distinguish them, we call the main ATLAS camera “acam” and the auxiliary camera “xcam.” The xcam data are not a mature data product and are not yet part of the ATLAS PDS bundle.

Based on experience from similar astronomical software projects (Pan-STARRS [2], LSST[3]), ATLAS chose to limit its exposure to modern, fast-moving software platforms and libraries, opting to base most of the pipeline processing in C (specifically C99) and GNU Bash version 4.3. Most of the high-performance, “heavy lifting” code is written as standalone C programs that operate on FITS images; these programs are orchestrated using collections of Bash scripts that compose the Reduction and Subtraction stages of the data processing pipeline.

Prior to the start of observations each night, the ATLAS telescope control system (TCS) performs a system “preflight” that ensures all facility components are functioning properly. Then, weather permitting, the TCS opens the dome automatically during twilight to obtain sky flatfield images and perform a focus run, and finally, at astronomical twilight, the pre-programmed science schedule begins.

Observing schedules are prepared automatically by custom ATLAS “wildsky” scheduling software during the local afternoon for each telescope. An ATLAS telescope schedule is an ordered sequence of fields to be observed through the night, each specified by the celestial coordinates (J2000.0 RA and Dec in decimal degrees) of the center of the field. Typically, ATLAS acquires four 30-second exposures of each field, spread over an interval of 0.5 – 1.0 hours. Optimizing such a schedule involves fitting in as many fields as possible and making sure they are observed with close to the nominal time spacing and in good sky position. This, in turn, means arranging the sequence so that the telescope and dome can move from each field to the next as quickly as possible: *i.e.*, minimizing moves that require long dome rotations or time-consuming meridian flips from the ATLAS telescope’s German equatorial mount.

ATLAS tiles the sky into a *tessellation* consisting of  $\sim 1720$  distinct “footprints”<sup>1</sup> that provide 100% sky coverage with minimal overlap. These footprints cover all points of the sky, including the Milky Way and both celestial poles.

A *wildsky* schedule rasters the sky in coarse bands of declination, avoiding observations within 10 deg of the moon when the moon’s brightness will interfere with observations. Otherwise, ATLAS observes all other parts of the sky, including the Milky Way and both celestial poles. The *wildsky* scheduler runs continuously during the night and adapts the remaining schedule for weather and other interruptions such as dedicated followup of a single important asteroid or troubleshooting of a minor problem. As with other NEO surveys, ATLAS executes repeat observations over the sky to detect moving objects. Each footprint in a night’s raster is scheduled for four visits over a 30-minute span so that moving objects can be detected by searching for sources moving linearly (generally) over the four exposures. A grouping of four detections that might be a moving object is called a “tracklet”, the fundamental unit of data submitted to the MPC.

Figure 1 shows the high-level view of the ATLAS data reduction pipeline. Each exposure is passed through four steps of the pipeline: reduction (image calibration), subtraction, the ATLAS moving object processing system (“MOPS”), and post-reduction. The reduction step produces a “standard” flattened, calibrated image from the raw camera file from the telescope. The reduction also corrects for electronic cross-talk artifacts between CCD amplifiers, and it computes a correction for clouds across the image. The cross-talk and cloud corrections are stored as image planes in the reduced FITS file. A complete ATLAS image reduction takes approximately 300 seconds to execute.

Subtraction removes the non-varying sky, mostly background stars and galaxies, leaving an image with true astronomical transient phenomena (moving objects, supernovae, active galaxy nuclei, etc.) and contaminants such as artificial satellites, optical ghosts and glints, CCD artifacts, and so on. Source-finding code operates on the subtracted image (or “difference image”) to create a per-exposure catalog of transient

---

<sup>1</sup>To reduce systematic errors that can occur when stars are always imaged on the same part of the detector, ATLAS employs 25 different tessellations that contain 1721 – 1725 footprints. A different tessellation is used each lunation.



01a59201o0019c	
01	ATLAS site (01=Maunaloa, 02=Haleakalā, 03=South Africa, 04=Chile)
a	Aperture identifier (a=acam, x=xcam, k=allsky)
01a	“Sitecam”, combination of site and aperture identifier
59201	Night number based on Modified Julian Day (e.g. Fri Dec 18 2020 UTC)
o	Exposure type (o=object, f=skyflat, s=focus, e=engineering)
0019	Per-telescope, per-night sequence number
c	Filter (c=cyan, o=orange)

Table 2: ATLAS observation name schema

Step	Description	In PDS Bundle
<code>sta1600</code>	Convert raw camera to calibrated FITS image; correct for cross-talk	Y
<code>impsf.sh</code>	Compute a PSF mosaic image (for quality control)	N
<code>imstars.sh</code>	Find suitable reference stars for astrometric calibration	N
<code>anet.sh</code>	Find astrometric solution using astrometry.net	N
<code>imphot.sh</code>	Compute a photometric calibration using reference stars	N
<code>imcloud.sh</code>	Compute an image-wide cloud correction	N
<code>impack.sh</code>	Produce complete multi-extension packed FITS image and 1/8 scale JPEG	Y

Table 3: `imred.sh` processing steps and their outputs.

sources. From a single exposure, it is generally impossible to tell if a given source is an asteroid, so ensembles of source catalogs at the same footprint are analyzed by MOPS to identify candidate moving objects. The post-reduction step performs a deep source detection using `dophot`[4] and other bookkeeping tasks that are not essential for NEO discovery. The orange boxes in the pipeline overview (Figure 1) represent data products that constitute the ATLAS PDS bundle: the reduced FITS image, its deep source catalog, the difference FITS image, and the difference source catalog. ATLAS image subtraction and source catalog generation typically takes 600-900 second to execute.

Each image taken by an ATLAS camera (either `acam` or `xcam`) is given a unique ATLAS observation name, sometimes called `obsname` or “obs”. The `obsname` encodes bookkeeping information useful for organizing exposures - the ATLAS site, aperture (camera), night identifier, type of exposure, filter, and a sequence number within the night. All processing files for a given exposure are prepended with its unique OBS name. The ATLAS night number is a local concept based on a Modified Julian Day (MJD) used to aggregate observations that occur within the same night at a particular telescope. While the instantaneous MJD is continuous, the night number is defined as an integer that remains the same all night, regardless of the offset of the site from UTC. The number chosen is the integer of the instantaneous MJD at the local midnight, and this night number is used for all observations within the noon-to-noon interval surrounding the local midnight.

For example, just after the local noon at ATLAS Maunaloa in Hawai‘i on Monday April 4 12:04:38 HST 2022, the UTC time is Monday April 4 22:04:39 UTC 2022 and the instantaneous MJD is 59673.9198727. At midnight, the MJD is about 0.5 larger, 59673.9198727, and the integer of this value is 59673 . Thus all ATLAS Maunaloa observations the evening of April 4 will have night number 59673.

## 4.2 Data Reduction

In the ATLAS PDS bundle, reduced data consists of files in the Flexible Image Transport System (FITS) format, or comma-separated value (CSV) text files. Currently, only ATLAS `acam` images and their associated source catalogs are included in the ATLAS PDS bundle. Figure 1 illustrates the high-level view of ATLAS data processing for a single `acam` exposure from a single telescope.

A reduced observation begins with a TCS-generated `OBS.inst` textual key-value instrumental parameter file describing per-observation essential details for a commanded exposure. This `OBS.inst` file has a FITS-like format for easy incorporation into subsequent FITS files. After the exposure completes, a raw device-

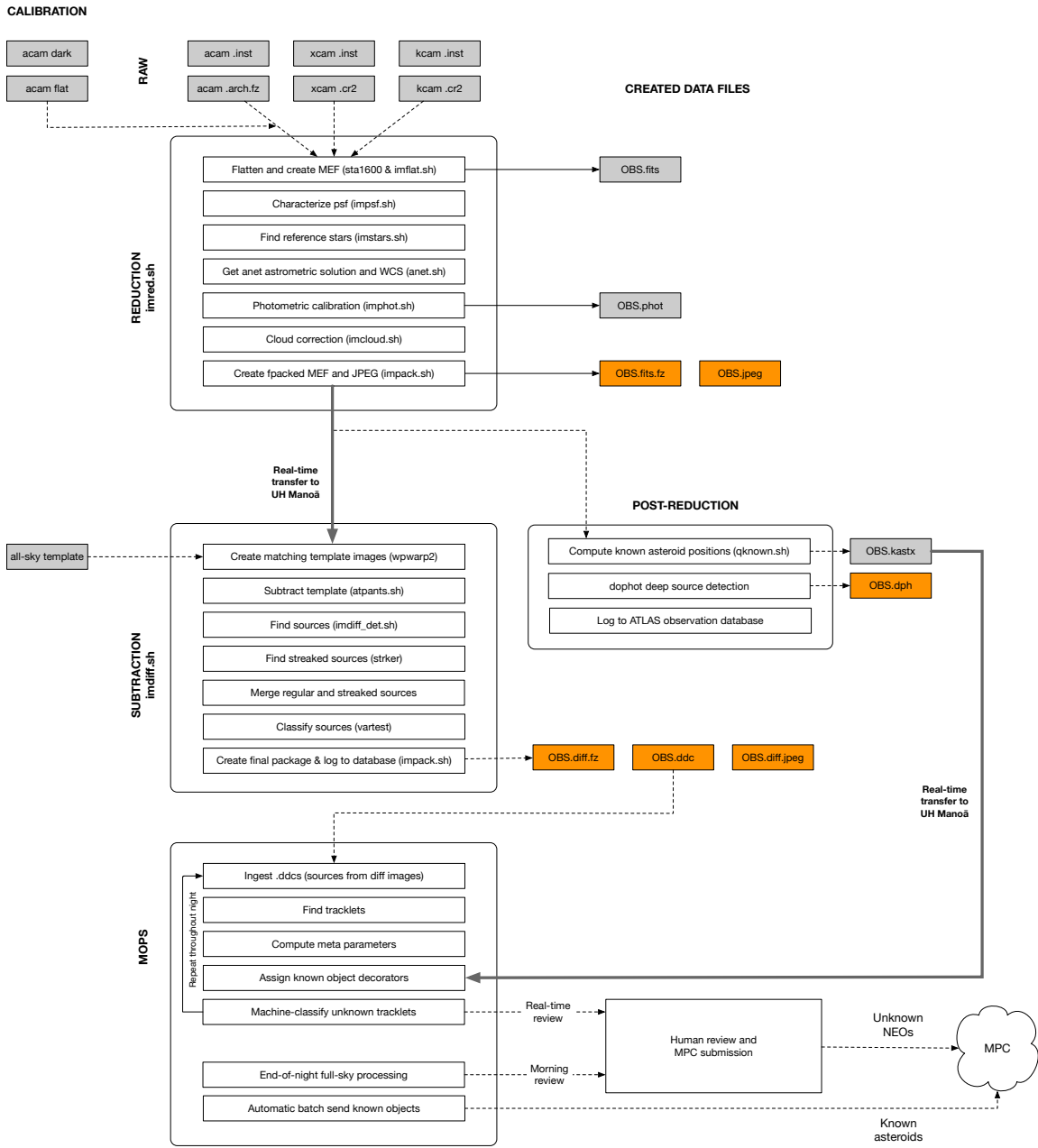


Figure 1: High-level ATLAS data processing flowchart. The orange boxes represent files that are present in the ATLAS PDS bundle.

dependent image file (called `OBS.arch.fz` for `acam`) is downloaded from the camera and saved to disk, then an image reduction is executed via a single script called `imred.sh`. The `OBS.inst` and `OBS.arch.fz` form the basic inputs to the image reduction pipeline. Additional global inputs include a dark and bias images, a bad pixel mask, and amplifier crosstalk corrections, and per-site per-camera reduction parameters. The final output of `imred.sh` is a photometrically and astrometrically calibrated image and auxiliary files detailing various steps of the reduction. A table of reduction steps and their availability in the PDS bundle is included in Table 4.

The workhorse of the image reduction step is the `sta1600` program, which converts a raw CCD image to a sky image. `sta1600` knows about device-specific details such as bad CCD pixels and columns, gain and bias differences between CCD amplifiers, and how pixels can be affected by inter-amplifier “crosstalk”. `sta1600` applies a full-image dark current and bias image correction, and creates a mask that identifies CCD defects and pixels that are likely unusable due to saturation or bright optical artifacts.

After `sta1600` runs, `impsf.sh` step runs to produce a composite image of “average” stars so that the telescope system’s point spread function (PSF) can be monitored. Next, `imstars.sh` finds stars in the image using the `dophot` source-finding program and cross-matches found stars with the ATLAS “refcat” star catalog [5]. `imstars.sh` strives to handle poorly-conditioned images that may have spatial gaps in star coverage due to clouds, galactic dust, or very-bright nearby sources. A typical ATLAS exposure will contain 30,000-50,000 reference stars.

Given a suitable catalog of reference stars for a single image, the astrometric solution, or precise sky coordinate system for the exposure including optical distortion, is computed using a modified version of `astrometry.net`[6] called `anet.sh`. ATLAS produces both distortion coefficients that comply with both the PV[7] and SIP[8] standards. Using the same catalog of reference stars, their reference magnitudes in various filter systems, and the bandpass of the exposure (usually cyan or orange), `imphot.sh` determines the photometric zeropoint of the image. The zeropoint is allowed to vary spatially across the exposure, and the subsequent `imcloud.sh` step computes the zeropoint correction across the exposure. Finally, `impack.sh` generates a binned-by-8 JPEG version of the full image suitable for viewing on a web page and packs all reduction components into an fpacked multi-extension FITS file (MEF) with extension `.fits.fz`. Details regarding the reduced MEF file can be found in the Bundle Overview document accompanying this document.

### 4.3 Image Subtraction

ATLAS finds asteroids by searching catalogs of sources from images that have the non-varying sky removed. We call the ATLAS full-sky pixel image of the non-varying sky the “wallpaper”. For every reduced image, a matching image from the wallpaper, called the template image, is extracted by the pipeline, and all stars and galaxies are subtracted at the pixel level, leaving only moving objects, variable stars, new stationary objects that have appeared since the generation of the wallpaper, and optical or electronic artifacts. The resulting image is called a ATLAS “difference image” and is stored in an fpacked FITS file with extension `.diff.fz`. The primary reasons to search for asteroids in subtracted images instead reduced images are to a) find asteroids in crowded fields, such as the galactic plane, and near bright stars; b) to detect asteroids moving in front of a relatively bright galaxy; c) to detect slow-moving objects that might resemble a star in an unsubtracted image; and d) to produce more accurate photometry for objects moving in front of a bright source. As long as the wallpaper template image has high enough signal-to-noise (at least  $\sim 10$  images in the wallpaper), no photometric precision is lost as a result of the image subtraction.

Image subtraction requires the reduced image to be of a minimum quality in order for the subtraction to be successful. Fundamentally the image should have a calibrated magnitude zeropoint, measured  $5 - \sigma$  limiting magnitude, and no significant loss of image due to clouds. If these are not true for a given image, the diff image will not be created.

ATLAS telescope scheduling is carefully produced to assist in the construction of high-quality wallpaper while satisfying basic observing requirements. The wallpaper is constructed by median-stacking images over the entire sky into a set of tiles that are later assembled on-the-fly into template images. The set of footprints that the scheduler raster the sky is altered each lunation so that the boundaries between footprints vary. This allows a particular patch of sky to be imaged over time at different places on the CCD, reducing systematic errors.

The image subtraction algorithm is an adapted version of `hotpants`[9], adapted to ATLAS images and

Step	Description	In PDS Bundle
<code>imdiff_diff.sh</code>	Retrieve wallpaper, register images, subtract, produce FITS file	Y
<code>imdiff_det.sh</code>	Search diff image for sources	N
<code>vartest</code>	Classify sources as real/spurious, produce catalog	Y

Table 4: `imdiff.sh` processing steps and their outputs.

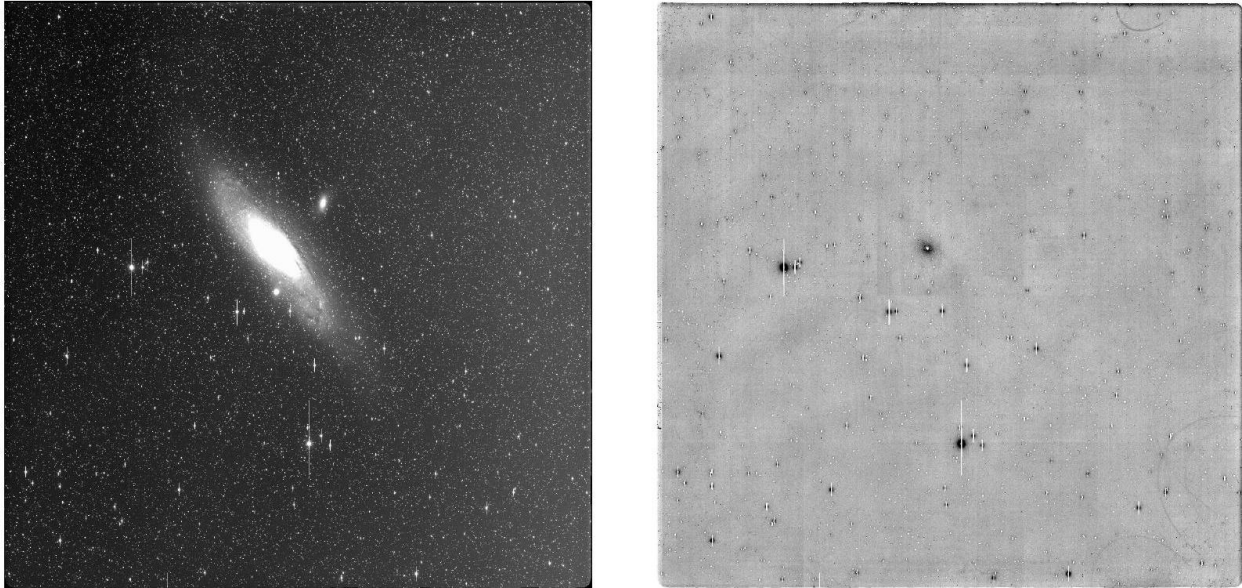


Figure 2: Reduced image 02a59618001280 (left) and its background-subtracted image (right). The `atpants`  $8 \times 8$  grid is faintly visible in the subtracted image.

called `atpants`. The primary ATLAS modifications to `hotpants` are the ability to read `fpacked` (compressed) FITS files, and comprehensive logging of subtraction processing statistics so that poor subtractions can be recognized. The original `hotpants` code has poorly understood (to us) failure modes when operating on wide-field images; these failure modes involve difficulty in finding “model” stars from which the PSF is estimated. The `atpants` adaptation subdivides a source image into an  $8 \times 8$  grid of subregions for PSF and sky analysis, leaving a low-level background pattern that is cosmetically unappealing but produces no notable degradation of photometry for sources on the boundaries between subregions. Figure 2 shows a reduced ATLAS image of galaxy M31 and its `atpants` subtracted image. Table 4 lists the high-level steps in an image subtraction.

After the static sky is subtracted, the `imdiff_det.sh` pipeline searches for sources in the difference image using the `tphot`[10] photometry code and produces a temporary table of sources found in the subtracted image. The detections from `imdiff_det.sh` are then curated by a detection classifier called `vartest` that attempts to label whether a given diff source detection is a moving object, stationary transient, or artifact based on the local pixel environment and what type of PSF was fitted. The inputs to `vartest` are the detection catalog from `imdiff_det.sh`, the complete diff and reduced images, and a file of bright stars in the image produced during the production of the reduced (unsubtracted) image earlier in the pipeline. Using all of this information, `vartest` decides whether a detection is likely to be a variable star, transient detection, cosmic ray, an image artifact such as bad pixel column or electronic crosstalk between amplifiers, or “scar” from a noisy star subtraction. The `vartest` outputs are combined with the diff detection catalog into the “final” source catalog for the diff image, called a “difference detection catalog” or `.ddc` file; sources in a `.ddc` file are called “transient detections”.

Especially important parameters in a `.ddc` file are the shape of the fitted PSF, likelihoods of matching various classes of transient detections, and a code describing whether the PSF was fitted one of various

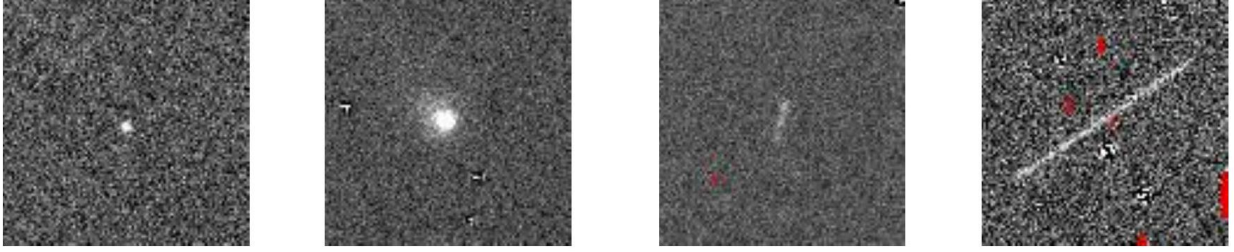


Figure 3: Sources fitted with different PSF models, from left to right: fixed (asteroid 2021 WX3), free (comet C/2020 M5 (ATLAS)), trailed (unknown asteroid), streaked (artificial satellite Z-3B DEB).

PSF models called *fixed*, *free*, *trailed* or *streaked*. Stars are fitted with the fixed PSF model (precisely, a “Waussian”[10], or 2-D Gaussian polynomial approximation truncated at the  $r^6$  term, that matches the stellar PSF model for an image), but moving objects may be fitted with the free, trailed or streaked PSF models. In the free model, PSF parameters are allowed to deviate slightly from a stellar profile. In trailed and streaked, sources must match stellar-shaped sources with slightly or extremely extended motion over the 30-second exposure. Figure 3 shows example sources fitted with the fixed, free, trailed and streaked PSF models. A full description of all .ddc columns is provided in the ATLAS bundle description document.

#### 4.4 Post-Reduction and Deep Source Detection

The post-reduction step is a catch-all step where some internal pipeline bookkeeping is handled and the `dophot`[4] deep source detection is invoked. The bookkeeping involves generation of calibration data for focus and engineering images, prediction of known asteroids likely to be in the exposure, and logging of the exposure to internal tables since the exposure reduction is now complete. After all bookkeeping is complete, the pipeline processes the reduced image with `imdophot.sh`, a deep source finder for stellar sources based on `dophot`. `dophot` performs exceptionally well on crowded fields where most source finders have difficulty. The motivation for including the `dophot` deep source output in the ATLAS PDS bundle is to recover photometry of solar system bodies that are unfound by the difference image processing pipeline that is optimized for NEOs. Example solar system objects that would be present in the `dophot` stream:

- main-belt asteroids in their stationary points where reflex motion against the stellar background is nearly zero
- asteroids that did not produce a 3- or 4-detection tracklet due to a lost exposure or intrinsic brightness variation
- very-distant asteroids whose motion over a four-exposure interval is very small and statistically equal to a stationary source, e.g. Kuiper Belt objects or a hypothetical Planet X

The output of `imdophot.sh` is a columnar text file that is described in detail in the ATLAS bundle description document. ATLAS-specific invocation parameters for `dophot` are described in Table 5.

#### 4.5 Asteroid Processing

ATLAS employs an adapted version of the Pan-STARRS Moving Object Processing System (MOPS)[11], a software system that identifies “tracklets” of source detections across multiple image catalogs that are likely to be moving objects. The details of MOPS are beyond the scope of this document; the ATLAS-specific modifications to the original system will be described in an upcoming paper. All asteroid tracklets are delivered to the IAU Minor Planet Center (MPC), either in real time via the MPC’s NEO Confirmation Page or a daily upload of known objects automatically identified by the MOPS pipeline. The MPC is the authoritative source for asteroid observations published by ATLAS.

Parameter	Description	Value
APRAD	Aperture radius in pixels (0=non-fixed)	0
FWHM	Externally provided FWHM in pixels (0=not provided)	0
VPSF	Polynomial order for variable PSF (0=fixed PSF)	0
BLUR	Blur image by specified FWHM in pixels (0=no blur)	0
BLOAT	Flag to “bloat” the PSF noise footprint (0=no bloat)	0
NSMIN	Terminate if NSMIN stars are found	10,000,000
NSMAX	Maximum number of stars allowed in image	3,000,000

Table 5: ATLAS `dophot` invocation parameters.  $NSMIN > NSMAX$  effectively instructs `dophot` to find as many stars as possible, up to  $NSMAX$ , and not to terminate its search earlier.

ATLAS asteroid processing occurs automatically following the completion of image subtraction. When the difference processing for the fourth exposure at a footprint is complete, MOPS begins a search for asteroids within the footprint. Detections that make up a moving object found by MOPS are called a “tracklet”. Tracklets created by MOPS are cross-matched with known objects predicted to be in each exposure. Tracklets matched with known asteroids account for the vast majority of objects detected each night by ATLAS. The astrometry and photometry for the matched known objects are submitted each morning in bulk to the MPC. Typical known object batches will contain data for tens of thousands of asteroids.

The remaining unmatched objects, presumed to be real objects and likely unknown near-Earth asteroids, must be screened by a human reviewer before they are submitted to the MPC NEO Confirmation Page. Human screening is necessary to prevent bogus tracklets from making it to the confirmation page; if this happens, other telescopes may spend precious telescope time chasing false positives.

During a typical night, humans will screen several dozen unknown object candidates, of which most will be recent discoveries that are not yet in the known object catalog, some will be bona fide NEO discoveries, and a handful will be bogus. The number of “raw” tracklets produced by each telescope each night can be in the thousands, but most of these are bogus tracklets generated by optical artifacts that happen to align linearly across the detections in a footprint. ATLAS deep machine learning code[12] has learned how to identify these, so the number of bogus tracklets that are seen by a reviewer is very small, a handful per night.

Authoritative identification of ATLAS tracklets to known objects is performed solely by the MPC. For this reason, these data are not part of the ATLAS PDS bundle; we refer users to the MPC catalogs and database for astrometry and photometry of submitted solar system objects.

## 4.6 Forced Photometry Server

The greater ATLAS collaboration operates the ATLAS Forced Photometry Server[13], a web service that can extract measurements of star-like sources at a specific location on the sky for the entire history of the ATLAS survey. “Forced” means that the position to be measured is precisely known by the user, and that the server software should attempt to measure an astronomical source at this sky location. The server uses each exposure’s parameters for how the point spread function (PSF) varies across the exposure to establish the PSF at the desired measurement location, and a sky flux is measured using this PSF model.

The ATLAS Forced Photometry Server can also produce measurements of asteroids and comets, provided that their orbits are good enough to generate ephemerides (predicted positions) at a one-pixel precision (about 2 arcseconds). In this mode, the user specifies the name of an asteroid or comet from the Minor Planet Center’s catalog, and the forced photometry server computes the position of this object in all ATLAS exposures. When the object is predicted to be in a particular exposure, the brightness of the object is measured in the same manner as a non-moving source.

## References

- [1] J. L. Tonry, L. Denneau, A. N. Heinze, B. Stalder, K. W. Smith, S. J. Smartt, C. W. Stubbs, H. J. Weiland, and A. Rest. ATLAS: A High-cadence All-sky Survey System. *Publications of the Astronomical Society of the Pacific*, 130(988):064505, 2018.
- [2] K. W. Hodapp, N. Kaiser, H. Aussel, W. Burgett, K. C. Chambers, M. Chun, T. Dombek, A. Douglas, D. Hafner, J. Heasley, J. Hoblitt, C. Hude, S. Isani, R. Jedicke, D. Jewitt, U. Laux, G. A. Luppino, R. Lupton, M. Maberry, E. Magnier, E. Mannery, D. Monet, J. Morgan, P. Onaka, P. Price, A. Ryan, W. Siegmund, I. Szapudi, J. Tonry, R. Wainscoat, and M. Waterson. Design of the Pan-STARRS telescopes. *Astronomische Nachrichten*, 325(6):636–642, October 2004.
- [3] Ž. Ivezić, S. M. Kahn, J. A. Tyson, B. Abel, E. Acosta, R. Allsman, D. Alonso, Y. AlSayyad, S. F. Anderson, J. Andrew, and et al. LSST: From Science Drivers to Reference Design and Anticipated Data Products. *The Astrophysical Journal*, 873:111, March 2019.
- [4] P. L. Schechter, M. Mateo, and A. Saha. DoPHOT, A CCD Photometry Program: Description and Tests. *Publications of the Astronomical Society of the Pacific*, 105:1342, 1993.
- [5] J. L. Tonry, L. Denneau, H. Flewelling, A. N. Heinze, C. A. Onken, S. J. Smartt, B. Stalder, H. J. Weiland, and C. Wolf. The ATLAS All-Sky Stellar Reference Catalog. *The Astrophysical Journal*, 867(2):105, 2018.
- [6] D. Lang, D. W. Hogg, K. Mierle, M. Blanton, and S. Roweis. Astrometry.net: Blind Astrometric Calibration of Arbitrary Astronomical Images. *The Astronomical Journal*, 139(5):1782–1800, 2010.
- [7] E. Bertin. Automatic Astrometric and Photometric Calibration with SCAMP. *Astronomical Data Analysis Software and Systems XV*, 351:112, 2006.
- [8] D. L. Shupe, M. Moshir, J. Li, D. Makovoz, R. Narron, and R. N. Hook. The SIP Convention for Representing Distortion in FITS Image Headers. *Astronomical Data Analysis Software and Systems XIV*, 347:491, 2005.
- [9] A. Becker. HOTPANTS: High Order Transform of PSF AND Template Subtraction. *Astrophysics Source Code Library*, ascl:1504.004, 2015.
- [10] S. Sonnett, K. Meech, R. Jedicke, S. Bus, J. Tonry, and O. Hainaut. Testing accuracy and precision of existing photometry algorithms on moving targets. *Publications of the Astronomical Society of the Pacific*, 125(926):456, April 2013.
- [11] Larry Denneau, Robert Jedicke, Tommy Grav, Mikael Granvik, Jeremy Kubica, Andrea Milani, Peter Vereš, Richard Wainscoat, Daniel Chang, Francesco Pierfederici, N. Kaiser, K. C. Chambers, J. N. Heasley, Eugene A. Magnier, P. A. Price, Jonathan Myers, Jan Kleyna, Henry Hsieh, Davide Farnocchia, Chris Waters, W. H. Sweeney, Denver Green, Bryce Bolin, W. S. Burgett, J. S. Morgan, John L. Tonry, K. W. Hodapp, Serge Chastel, Steve Chesley, Alan Fitzsimmons, Matthew Holman, Tim Spahr, David Tholen, Gareth V. Williams, Shinsuke Abe, J. D. Armstrong, Terry H. Bressi, Robert Holmes, Tim Lister, Robert S. McMillan, Marco Micheli, Eileen V. Ryan, William H. Ryan, and James V. Scotti. The Pan-STARRS Moving Object Processing System. *Publications of the Astronomical Society of the Pacific*, 125(926):357, April 2013.
- [12] Amandin Chyba Rabeendran and Larry Denneau. A Two-stage Deep Learning Detection Classifier for the ATLAS Asteroid Survey. *Publications of the Astronomical Society of the Pacific*, 133(1021):034501, March 2021.
- [13] K. W. Smith, S. J. Smartt, D. R. Young, J. L. Tonry, L. Denneau, H. Flewelling, A. N. Heinze, H. J. Weiland, B. Stalder, A. Rest, C. W. Stubbs, J. P. Anderson, T. W. Chen, P. Clark, A. Do, F. Förster, M. Fulton, J. Gillanders, O. R. McBrien, D. O’Neill, S. Srivastav, and D. E. Wright. Design and Operation of the ATLAS Transient Science Server. *Publications of the Astronomical Society of the Pacific*, 132(1014):085002, August 2020.